Gut microbiota depletion affects nutritional and behavioral responses to activity-based anorexia model in a sex-dependent manner

Pauline Tirelle, Jonathan Breton, Alexandre Kauffmann, Wafa Bahlouli, Clément L'Huillier, Emmeline Salameh, Asma Amamou, Marine Jarbeau, Charlène Guérin, Alexis Goichon, et al.

▶ **To cite this version:**

Pauline Tirelle, Jonathan Breton, Alexandre Kauffmann, Wafa Bahlouli, Clément L'Huillier, et al.. Gut microbiota depletion affects nutritional and behavioral responses to activity-based anorexia model in a sex-dependent manner. Clinical Nutrition, 2021, 40 (5), pp.2734-2744. 10.1016/j.clnu.2021.04.014 . hal-03254828

HAL Id: hal-03254828

https://normandie-univ.hal.science/hal-03254828v1

Submitted on 9 May 2023

HAL is a multi-disciplinary open access archive for the deposit and dissemination of scientific research documents, whether they are published or not. The documents may come from teaching and research institutions in France or abroad, or from public or private research centers.

L'archive ouverte pluridisciplinaire **HAL**, est destinée au dépôt et à la diffusion de documents scientifiques de niveau recherche, publiés ou non, émanant des établissements d'enseignement et de recherche français ou étrangers, des laboratoires publics ou privés.

Distributed under a Creative Commons Attribution - NonCommercial 4.0 International License

Version of Record: https://www.sciencedirect.com/science/article/pii/S0261561421002065
Manuscript_9993f5be1a19aacf1ffb77ff3f0c60aa

Gut microbiota depletion affects nutritional and behavioral responses to activity-based anorexia model in a sex-dependent manner.

Pauline Tirelle[1,2], Jonathan Breton[1,2,3], Alexandre kauffmann[1,2], Wafa Bahlouli[1,2], Clément L'Huillier[1,2], Emmeline Salameh[1,2], Asma Amamou[1,2], Marine Jarbeau[1,2], Charlène Guérin[1,2], Alexis Goichon[1,2], Jean-Claude do Rego[2,4], Pierre Déchelotte[1,2,3], David Ribet[1,2], Moïse Coëffier[1,2,3]

[1] Normandie University, UNIROUEN, INSERM UMR 1073 "Nutrition, inflammation and gut-brain axis", Rouen, France

[2] Institute for Research and Innovation in Biomedicine (IRIB), UNIROUEN, Rouen, France

[3] Department of Nutrition, Rouen University Hospital, Rouen, France

[4] Animal Behavior Facility, SCAC, UNIROUEN, France

*Corresponding author: Moïse Coëffier - INSERM U1073, UFR Santé, 22 boulevard Gambetta, 76183 ROUEN cedex France – tel +33235148240; moise.coeffier@univ-rouen.fr

Word count: 5,225

© 2021 published by Elsevier. This manuscript is made available under the CC BY NC user license
https://creativecommons.org/licenses/by-nc/4.0/

Abstract:

Background & aims: In the last decade, the role of the microbiota-gut-brain axis in eating behavior and anxiety-depressive disorders has gained increasing attention. Although a gut microbiota dysbiosis has been reported in anorectic patients, its pathophysiological role remains poorly understood. Thus, we aimed to characterize the potential role of gut microbiota by evaluating the effects of its depletion in the Activity-Based Anorexia (ABA) mouse model both in male and female mice.

Methods: Male and female C57Bl/6 mice were submitted (ABA group) or not (CT group) to the ABA protocol, which combines access to a running wheel with a progressive limited food access. Gut microbiota was previously depleted or not by a cocktail of antibiotics (ATB) delivered by oral gavages. We monitored body composition, anxiety-like behavior, leptin and adiponectin plasma levels, hypothalamic and hippocampal neuropeptides mRNA levels, as well as dopamine (DRD) and serotonin (5HT1 and 4) receptors mRNA expression.

Results: In response to the ABA model, the body weight loss was less pronounced in ATB-treated ABA compared to untreated ABA, while food intake remained unaffected by ATB treatment. ATB-treated ABA exhibited increased fat mass and decreased lean mass compared to untreated ABA both in male and female mice, whereas but plasma adipokine concentrations were affected in a sex-dependent manner. Only male ABA mice showed a reduced anticipatory physical activity in response to ATB treatment. Similarly, anxiety-like behavior was mainly affected in ATB-treated ABA male mice compared to ATB-treated ABA female mice, which was associated with male-specific alterations of hypothalamic CRH mRNA and hippocampal DRD and 5-HT1A mRNA levels.

Conclusions: Our study provides evidence that ATB-induced gut microbiota depletion triggers alterations of nutritional and behavioral responses to the activity-based anorexia model in a sex-dependent manner.

Keywords: anorexia; gut microbiota; gut brain axis; anxiety-like behavior; activity-based anorexia

1. Introduction:

Anorexia Nervosa (AN) is an eating disorder described by the Diagnostic and Statistical Manual of Mental Disorders fifth edition (DSM-V)[1] and is the mental illness with the highest mortality rate[2], which makes it a major public health problem. AN is a multifactorial disease with female predominance, the lifespan prevalence being 1.4% for women and 0.2% for men[3]. AN is characterized by an undernutrition (body mass index (BMI) < 18.5 kg/m^2), an intense fear of gaining weight and disturbance in body shape perception. Psychiatric comorbidities such as anxiety and depression are frequently observed[4]. AN is a multifactorial disease with biological, psychological, environmental and social influences[5].

Over the last decade, the role of the gut-brain axis in the regulation of eating behavior[6] and anxiety-depressive disorders[7] has emerged. Indeed, the role of the gut microbiota on host satiety has been highlighted[8] and gut microbiota dysbiosis (abundance and diversity) has been reported in anorectic patients[9] [10]. Furthermore, it has been suggested that modifications of gut microbiota in anorectic patients are associated with BMI[11] and body composition[12], and are not completely restored after refeeding[13]. Interestingly, preliminary studies and case reports evaluating fecal microbiota transplantation underlined putative role of gut microbiota in the regulation of energy homeostasis during AN[14,15,16]. Finally, the gut microbiota also affects mood disorders, particularly anxiety-depressive disorders. Indeed, patients with anxiety-depressive disorders exhibited gut microbiota dysbiosis[17] and fecal microbiota transplantation from depressive patients to germ-free animals was associate with the occurrence of altered behaviors[18]. In addition, Neufeld *et al* reported reduced anxiety-like behavior and altered neurochemical pathways in amygdala and hippocampus in germ-free mice[19].

Among animal models used to decipher the pathophysiology of eating disorders and particularly to mimic AN, the activity-based anorexia (ABA) model is one of the most commonly used[20]. It combines a free access to a running wheel and a progressive food access limitation. It leads to a severe body weight loss, an early physical hyperactivity, and alterations in brain structures involved in eating

behavior[21,22] and anxiety disorders[23,24]. In addition, ABA mice exhibited inflammation[25] and an intestinal hyperpermeability[26]. Recently, we characterized the gut microbiota alteration occurring in ABA mice and observed similarities with the dysbiosis observed in AN patients[27]. The physiological consequences of these gut microbiota alterations during ABA remain however unknown.

Thus, we aimed to characterize the effects of gut microbiota depletion during the ABA model. As differential responses were observed in the ABA model according to the sex[28], we included both male and female mice in our study. As gut microbiota contributes to the intestinal immune system maturation[29], gut microbiota depletion was achieved by antibiotics treatments[30]. We then monitored body weight, food intake, physical activity and evaluated body composition, anxiety-like behavior, central neuropeptide response and intestinal parameters such as intestinal permeability.

2. Material and Methods:

2.1. Animals

Animal experiment was approved by the regional ethical committed CENOMEXA (authorization N/05-11-12/28/11-15). Experiments were carried out in accordance with current French and European regulations. Seven weeks old male and female C57BL/6Jrj mice (Janvier Labs, Le-Genest-Saint-Isle, France) were acclimated and housed at 23°C±2°C on reverse cycle (dark phase from 10:00 am to 10:00 pm), with water and food free-access (n=4 / cage). Animals were assigned randomly to various experimental groups.

2.2. Antifungal-antibiotics treatment

To deplete gut microbiota, mice received a cocktail of antifungal and antibiotics (ATB) in water until the end of the experiment by oral gavages (10µL/g of body weight) twice a day (d) as previously described[30]. Briefly, from d1 to d3, only antifungal treatments were performed by supplying 0.1mg/mL amphotericin-B (Sigma-Aldrich, Saint-Louis, MO, USA). Then, an antibiotic mixture

(Vancomycin 5 mg/mL, Neomycin 10 mg/mL, Metronidazole 10 mg/mL, Ampicillin 10 mg/mL) completed the treatment until the end of the protocol. Untreated mice received water by gavages.

2.3. Activity-based anorexia (ABA) model

At the beginning of the ABA procedure (d10), mice were placed individually in standard cage (CT and CT+ATB groups) or cages with an activity wheel (ABA and ABA+ATB groups). The ABA model has been performed as previously described[26]. ABA model combines a free running wheel access and a progressively limited food access from 6h/day to 3h/day (Supplemental Fig. S1). Food was given at the beginning of dark phase (10:00 am). Animals had free access to water. Running wheel activity has been continuously recorded with Activity Wheel software (Intellibio, Seichamps, France). Moreover, food intake and body weight were daily measured. If body weight loss was higher than 20% on 3 consecutively days, animals were euthanized in accordance with the ethical procedure.

2.4. Body composition

At d13 (before the limitation of food access) and d27 (end of the protocol), body composition was assessed on vigil animals using Minispec LF110 (Brucker, Wissembourg, France), a fast-nuclear magnetic resonance method (n= 8/6 for male and female).

2.5. Open field test

In order to assess anxiety-like behavior, Open Field tests were performed at d13 and d27 after the feeding period (at 01:00 pm) (n= 8/6 for male and female). Data were collected with Fusion Software (Omni-Tech Electronics, Eckington, UK).

2.6. Quantification of faecal bacterial density flow cytometry

The efficiency of gut microbiota depletion was assessed by quantifying the decrease of bacterial density in mouse faeces using flow cytometry, as previously described[30]. Briefly, faecal suspensions

were stained with Syto™ BC (Molecular Probes, Eugene, OR, USA) and fixed in 1X PBS-0.5% paraformaldehyde before being analysed by flow cytometry[30].

2.7. Euthanasia and sample collection

Mice were anesthetized by intraperitoneal injection of Ketamine/Xylazine solution (40 and 1 mg/kg of body weight, respectively). Blood was sampled by puncture in the portal vein and plasma samples were then collected after centrifugation (3000 g; 20 min; 4°c). Brain was removed in order to isolate hypothalamus and hippocampus. Colon was collected and immediately washed with ice-cold PBS, 1 cm-long sections were then performed and frozen in liquid nitrogen. All samples were stored at -80°C until analysis.

2.8. Intestinal permeability assessment

Global intestinal permeability was assessed by administration of a solution of *fluorescein isothiocyanate-Dextran* (FITC-Dextran 4 kDa) at 40 mg/mL by oral gavage (10 µL/g of body weight), 3 hours before euthanasia, as previously described [31]. Then, FITC-Dextran level was then measured on plasma samples using a spectrofluorometer (Chameleon Lablogic, Sheffield, UK; excitation = 485 nm; emission = 535 nm; Mikro Win 2000 Software).

2.9. Evaluation of plasma leptin, adiponectin and corticosterone

Plasma leptin and adiponectin levels were assessed using MILLIPLEX assay (Merckmillipore, Fontenay sous Bois, France) or enzyme-like immunosorbent assay (Invitrogen, Carlsbad, CA, USA), both according to the manufacturer's instructions. Plasma corticosterone levels were measured by a Corticosterone ELISA kit (Abnova, Ann Arbor, MI, USA) according to the manufacturer's instructions.

2.10. RNA extraction and RT-qPCR

Total hypothalamus, hippocampus and colonic RNAs were extracted by Trizol method (Invitrogen, Carlsbad, CA, USA) following manufacturer's guidelines. After DNAse treatment (Promega, Charbonnières-les-Bains, France), RNAs were reverse transcribed as previously reported[8]. Then, qPCR was performed using SYBRGreen technology on a Bio-Rad CFX96 real-time PCR system (Bio-Rad Laboratories, Marnes la Coquette, France). RPS18 gene was used as a housekeeping gene. Specific primer sequences of targeted mouse genes are displayed in **Table 1**. The values were obtained by the conversion of cycle threshold on concentration value by using a standard curve.

2.11. Statistical analysis

All data were analysed using GraphPad Prism 6.0 software (GraphPad Software Inc., San Diego, CA, USA). Data were expressed as mean ± standard error to mean. Shapiro test was used to assess distribution parameters. Data were analysed by repeated two-way ANOVA (time x group) or two-way ANOVA (ABA x ATB) followed by Bonferroni posthoc tests, as appropriate. Results were considered significant when p-value was lower than 0.05.

3. Results:

3.1. Impact of gut microbiota depletion during activity-based anorexia in male mice.

In order to control the efficiency of the ATB-mediated gut microbiota depletion, we compared bacteria abundance in faeces obtained before and after 15 days of ATB treatment. We observed a strong decrease in faecal bacterial density at day 15 (98% of depletion, Fig. 1), indicating that the gut microbiota is efficiently depleted before starting the ABA procedure.

At d13 (*i.e.* before the limitation of food access), we observed that gut microbiota depletion did not induce body weight changes in any groups (Supplemental Fig. S2A). Mice with access to an activity wheel exhibited a decreased fat mass (Supplemental Fig. S1B). Furthermore, ATB treatment induced an increase of fat mass (Supplemental Fig. S2B) and a decrease of lean mass (Supplemental

Fig. S2C). We also evaluated mice behavior and did not observe major effects of ATB treatment (Supplemental Fig. S2D-I), which was only associated with a reduction of the distance travelled at the centre of open-field system (Supplemental Fig. S2E).

Then, we started to decrease food access and followed-up mice until day 28. In CT mice, ATB treatment affected neither food intake nor body weight until day 28. As previously reported [26], ABA mice exhibited a decrease of food intake (data not shown), which is associated to a marked decrease of body weight at day 28 (15.2% compared to day 16, Fig. 2A, B). Interestingly, the body weight loss was less pronounced in ATB-treated ABA mice (10% compared to day 16) compared to untreated ABA mice (Fig. 2A, B), while food intake remained unchanged (data not shown). In response to ABA model, mice exhibited a modification of body composition with a reduction of both fat (-27%) and lean masses (-20%, Fig. 2C, D). Accordingly, plasma leptin markedly decreased in ABA mice (Fig. 3A), while adiponectin remained unaffected (Fig. 3B). In ATB-treated mice, we observed higher fat mass and lower lean mass, as already observed before the limitation of food access, both in CT and ABA. Indeed, ATB-treated CT mice showed an increase of fat mass of approximately 60% and a decrease of lean mass of 15% compared to untreated CT mice, whereas ATB-treated ABA mice exhibited an increase of 79% in fat mass and a decrease of 16% in lean mass compared to untreated ABA mice (Fig. 2C, D). ATB did not affect plasma leptin neither in CT nor in ABA mice (Fig. 3A), but increased plasma adiponectin level (ANOVA p (ATB) < 0.05, Fig 3B). In accordance with the absence of modification in food intake in ATB-treated ABA mice, hypothalamic NPY and POMC mRNA levels were not modified by ATB treatment in ABA mice (Fig. 4 A, B). Nevertheless, the increase of anticipatory physical activity was less pronounced in ATB-treated ABA mice compared to untreated ABA mice (Fig. 2E).

As we and others previously reported that intestinal permeability is affected either during ABA model[26] or in response to ATB treatment[33], we measured intestinal permeability in our model.

We observed that intestinal permeability was not significantly modified in male mice in our tested conditions (Fig. 3C).

We then focused on anxious behavior that was assessed at day 27. ABA mice exhibited altered behavior compared to CT mice: the distances travelled by mice at the center and at the periphery of the open field area were decreased while the time spent in these two areas remained unchanged. Consequently, the ratio distance / time decreased both at the center and at the periphery (Fig. 5 A-E). In addition, immobility time was increased in ABA mice compared to CT mice (Fig. 5G). ATB-induced gut microbiota depletion was associated with a more pronounced decrease of the travelled distance and of the ratio distance / time at the periphery in ABA mice compared to untreated ABA mice (Fig. 5E, F). A similar trend was observed at the center but difference did not reach significance (Fig. 5B). Interestingly, this effect was not observed in ATB-treated CT mice. In addition, ATB-treated ABA mice exhibited a reduced vertical activity compared to other groups (Fig. 5H). Plasma corticosterone remained unchanged (data not shown), while the increase of hypothalamic CRH mRNA observed in untreated ABA mice was totally blunted by ATB treatment (Fig. 5I). Hypothalamic TNFα and TLR4 mRNA levels were not modified (data not shown). In the hippocampus, we evaluated dopaminergic and serotoninergic systems by assessing dopamine and serotonin receptors. For DRD1, DRD2 and 5-HT1A (Htr1a gene), the ANOVA p-value for interaction was significant while there was no difference for 5-HT4 (Htr4 gene, Fig. 6A-D). Our data suggest that ATB treatment blunted the increase of DRD1 and DRD2 mRNA in ABA mice compared to CT (Fig. 6A, B). A similar pattern was also observed for TNFα mRNA (Fig. 6E) By contrast, 5-HT1A mRNA level was only decreased in ATB-treated ABA mice compared to ATB-treated CT mice but not in untreated ABA mice (Fig. 6C). Finally, BDNF mRNA levels remained unchanged (Fig. 6F).

3.2. Impact of gut microbiota depletion during activity-based anorexia in female mice.

As the prevalence of anorexia nervosa is higher in females than in males [34] and as mice exhibit sex-dependent differential responses to the ABA model [28], we thus decided to perform similar experiments in female mice.

As observed in males, ATB treatment led to a marked depletion of bacteria in mouse faeces (95% of depletion, Supplemental Fig. S3) with no impact on body weight but an increase of fat mass and a reduction of lean mass (Supplemental Fig. S4A-C). ATB treatment did not markedly affect female behavior, as we only observed a decrease of the time spent at the center of the open field area without any difference for the other measured parameters (Supplemental Fig. S4D-I).

After the beginning of the food access limitation, ABA female mice exhibited a body weight loss until day 22 (-21.7% vs day 16), but then partially recovered at day 28 (-11.1% vs day 16, Fig. 7A), as previously reported [21]. ATB-treated ABA mice exhibited a limitation of the body weight loss until day 22 compared to untreated ABA mice (-12.1% vs day 16, $p<0.05$, Fig. 7A). However, at day 28, body weight change was not different between ATB-treated and untreated ABA female mice (Fig. 7B). As observed in male mice, ATB affected body composition with an increase of fat mass and a decrease of lean mass in female mice submitted to the ABA model (Fig. 7C, D). However, plasma leptin and adiponectin concentrations were lower in ATB-treated ABA mice compared to untreated ABA mice (Fig. 8A, B). Food intake was reduced in ABA mice compared to CT mice, but was not affected by ATB treatment (data not shown) that was in agreement with the observed hypothalamic mRNA levels for NPY and POMC (Supplemental Fig. S5). In contrast to male mice, ATB-treated ABA female mice developed a similar anticipatory physical activity compared to untreated ABA mice (Fig. 7E). We did not observe any major effects of ATB treatment on female behavior at the end of the ABA protocol. Indeed, although ABA protocol induced a decrease of the distance travelled at the periphery of the open field area, an increase of immobility time and a decrease of vertical activity, ATB-treated ABA female mice did not exhibit exacerbated or blunted behavior compared to untreated ABA mice (Fig. 9 A-G). Accordingly, ATB treatment affected neither plasma corticosterone

(data not shown) nor hypothalamic CRH mRNA expression (Fig. 9I) nor hippocampal dopaminergic and serotoninergic receptors mRNA levels (Supplemental Fig. S6). Finally, ATB-treated ABA female showed a marked increase of intestinal permeability compared to untreated ABA mice and ATB-treated CT mice (Fig. 8C) that was not observed in male mice.

4. Discussion:

Recent data suggest that the gut microbiota contributes to the pathophysiology of eating disorders and particularly of AN[10]. Gut dysbiosis has been described in AN patients before and after refeeding[35]. These data have also been observed in ABA model both in rats[36] and mice[27]. Indeed, in a recent study, we characterized the gut microbiota alterations occurring in ABA mice[27] and observed some similarities with the dysbiosis reported in AN patients. We thus aimed to evaluate the contribution of gut microbiota in the ABA model, by monitoring the consequences of antibiotics-induced depletion. We report that antibiotics-induced gut microbiota depletion induces a similar modification of body composition in female and male mice, is associated with a limitation of body weight loss in the activity-based anorexia model in both sexes, but triggers a sex-dependent alteration of anxiety-like behavior.

Before the progressively time-limited food access, voluntary activity induced a sex-dependent modification in body composition of untreated mice. In contrast, antibiotics-induced gut microbiota depletion similarly induced an increase of adiposity and a reduction of lean mass in both sexes. Of note, body weight remained unaffected by antibiotics in accordance with previous data showing that different antibiotics cocktails, did not affect body weight both in female[37] and male[38, 39] mice and Siberian hamsters[40].

By contrast, after the beginning of the food access limitation, mice with depleted microbiota exhibit a less pronounced body weight loss compared to untreated mice. This effect was observed in

both female and male mice, even if it seems to be more pronounced in males. As observed before the limited food access, antibiotics treatment was associated with an increase of fat mass and a decrease of lean mass in response to the ABA mocel whatever the sex. To our knowledge, our study shows for the first time that gut microbiota depletion induced by antibiotics limits body weight loss during ABA model in both female and male mice. Contradictory data have been shown in germ-free mice that are less able to survive to starvation[41]. In the present study, we did not observe modification of food intake between untreated and antibiotics-treated mice, also during ABA model.

Concerning body composition, antibiotics treatment was associated with a reduction of muscle mass in male mice[38]. Similar data have been observed in germ-free male mice[42]. However, in those studies, the authors did not report on the amount of fat mass. By contrast, in female mice, antibiotics in early life did not affect lean mass but increased adiposity[37]. However, to our knowledge, the comparison of the effects of gut microbiota depletion on body composition between female and male mice remain until now undocumented. In Siberian hamsters, Sylvia *et al* studied the sex-specific modulation of microbiota in body weight, but did not assess body composition[40]. As previously reported[28], female and male mice exhibit different responses during ABA model. Indeed, in females, body weight loss was maximal at day 22, and then mice recovered that contributes to hide the differences between antibiotics-treated and untreated mice, and may explain the increased adiposity in female ABA mice compared to controls. By contrast, in males, the body weight loss persists until the end of protocol. In the present study, we thus demonstrated that antibiotics treatment increased adiposity and reduced lean mass in young adult mice in a sex-independent manner.

Anxiety and depression are frequent comorbidities during anorexia nervosa[43, 44] and the role of microbiota-gut-brain axis in these comorbidities has been suggested[45]. Interestingly, mice receiving the transplantation of gut microbiota from patients with anxiety exhibit anxious behavior[46], suggesting that the microbiota can be involved in psychiatric comorbidities in anorectic patients. In our study, before the limitation of food access, antibiotics treatment was not associated with major

modification of behavior of female and male mice placed in standard cages or in cages equipped with an activity wheel. We only observed a decrease of the distance travelled at the center of the open field area in male mice. At the end of ABA model, only male mice showed an altered behavior in response to antibiotics treatment. Indeed, the distance travelled at the periphery of the open field area was reduced in antibiotics-treated male mice. We observed a statistical antibiotics effect (2-way ANOVA) suggesting an increased immobility time, which is in consistent with the observed decrease of vertical activity. Along the same line, anticipatory physical activity was reduced in antibiotics-treated male mice compared to untreated mice. Finally, antibiotics treatment completely blunted the increase of hypothalamic CRH mRNA expression in response to ABA model. These alterations were not all present in female mice. Previous data focusing on broad-spectrum antibiotics showed that long-term exposure to ceftriaxone reduced both anxiety and aggressive behavior in male BALB/c mice[47]. By contrast, ampicillin administration increased anxiety and immobility in male BALB/c mice[39]. In Siberian hamsters, aggressive behavior was reduced by enrofloxacin in both females and males but only male animals restored it to control level after stopping treatment[40]. In humans, antibiotics exposure led in contrast to an increased risk to develop anxiety-like behaviors[48]. These behavioral changes were associated with gut microbiota alterations[40, 47, 39]. Interestingly, anxiety-like behavior has also been studied in germ-free animals. The absence of microbiota was associated with an anxiolytic behavior both in female[19] and male[48] germ-free mice. To our knowledge, we showed here for the first time that gut microbiota depletion induced by antibiotics alters the behavioral response to ABA model but only in male mice. Previous data reported gut microbiota dysbiosis in response to ABA[36, 27, 49] but it is interesting to note that these data have been obtained in male[36] and female[49] rats and in male mice[27]. It may be interesting to further compare gut microbiota alterations between male and female mice in response to ABA model. The underlying mechanisms or microbiota metabolites involved in the microbiota-gut-brain axis remain to be studied during the ABA model. Faecal and plasma metabolome has recently been described in response to the ABA model, but only in female mice[50]. We can speculate that several metabolites such as short-chain fatty acids, indole or

ClpB could be involved[51]. Indeed, it was recently reported that in response to a chronic stress, indole increased emotional responses[52] and that the bacterial ClpB protein, a mimetic of αMSH neuropeptide, contributed to the response to the ABA model[53]. To better understand the central regulation of behavior in our conditions, we studied dopaminergic and serotoninergic systems in the hippocampus by evaluating mRNA levels of their receptors, as well as TNFα and BDNF. Again, we only observed a response to antibiotics treatment during ABA model in male mice. Indeed, for DRD1, DRD2, 5HT1R and TNFα, a statistical interaction between ABA and antibiotics (2-way ANOVA) was observed. ABA-induced increases of DRD1, DRD2 and TNFα were blunted by antibiotics. The role of these alterations in the behavioral changes during ABA model remains to be further studied. In female mice, antibiotics did not affect these parameters in response to ABA model. The role of sex hormones that were able to affect bacterial ClpB protein levels or other bacterial metoabolites in response to host starvation[54] should be deciphered.

In conclusion, we report here for the first time that antibiotics-induced gut microbiota depletion limits body weight loss and modifies body composition in response to the ABA model, in a similar manner in female and male mice. By contrast, gut microbiota depletion affects behavioral responses to the ABA model only in male mice. We anticipate that our results will pave the way for further studies aiming at better understanding the underlying mechanisms and at targeting gut microbiota in order to improving different facets of anorexia pathophysiology.

5. Acknowledgements

This work was co-supported by the Microbiome foundation, the Roquette foundation for health and by European Union and Normandie Regional Council. Europe gets involved in Normandie with European Regional Development Fund (ERDF). PT received the support of the university of Rouen

Normandy during her PhD. These funders did not participate in the design, implementation, analysis, and interpretation of the data.

6. References:

1. Mitchell, J. E., Cook-Myers, T. & Wonderlich, S. A. Diagnostic criteria for anorexia nervosa: Looking ahead to DSM-V. *Int. J. Eat. Disord.* **37**, S95–S97 (2005).
2. Gravina, G., Milano, W., Nebbiai, G. & Capasso*, C. P. and A. Medical Complications in Anorexia and Bulimia Nervosa. *Endocrine, Metabolic & Immune Disorders - Drug Targets* http://www.eurekaselect.com/162598/article (2018).
3. Galmiche, M., Déchelotte, P., Lambert, G. & Tavolacci, M. P. Prevalence of eating disorders over the 2000–2018 period: a systematic literature review. *Am. J. Clin. Nutr.* **109**, 1402–1413 (2019).
4. Junne, F. *et al.* The relationship of body image with symptoms of depression and anxiety in patients with anorexia nervosa during outpatient psychotherapy: Results of the ANTOP study. *Psychotherapy* **53**, 141–151 (2016).
5. Arcelus, J., Witcomb, G. L. & Mitchell, A. Prevalence of eating disorders amongst dancers: a systemic review and meta-analysis. *Eur. Eat. Disord. Rev. J. Eat. Disord. Assoc.* **22**, 92–101 (2014).
6. van de Wouw, M., Schellekens, H., Dinan, T. G. & Cryan, J. F. Microbiota-Gut-Brain Axis: Modulator of Host Metabolism and Appetite. *J. Nutr.* **147**, 727–745 (2017).
7. Clarke, G. *et al.* The microbiome-gut-brain axis during early life regulates the hippocampal serotonergic system in a sex-dependent manner. *Mol. Psychiatry* **18**, 666–673 (2013).
8. Breton, J. *et al.* Gut Commensal E. coli Proteins Activate Host Satiety Pathways following Nutrient-Induced Bacterial Growth. *Cell Metab.* **23**, 324–334 (2016).
9. Morita, C. *et al.* Gut Dysbiosis in Patients with Anorexia Nervosa. *PLOS ONE* **10**, e0145274 (2015).
10. Breton, J., Déchelotte, P. & Ribet, D. Intestinal microbiota and Anorexia Nervosa. *Clin. Nutr. Exp.* **28**, 11–21 (2019).

11. Million, M. *et al.* Correlation between body mass index and gut concentrations of Lactobacillus reuteri , Bifidobacterium animalis , Methanobrevibacter smithii and Escherichia coli. *Int. J. Obes.* **37**, 1460–1466 (2013).
12. Mörkl, S. *et al.* Gut microbiota and body composition in anorexia nervosa inpatients in comparison to athletes, overweight, obese, and normal weight controls. *Int. J. Eat. Disord.* **50**, 1421–1431 (2017).
13. Mack, I. *et al.* Is the Impact of Starvation on the Gut Microbiota Specific or Unspecific to Anorexia Nervosa? A Narrative Review Based on a Systematic Literature Search. *Curr. Neuropharmacol.* **16**, 1131–1149 (2018).
14. de Clercq, N. C., Frissen, M. N., Davids, M., Groen, A. K. & Nieuwdorp, M. Weight Gain after Fecal Microbiota Transplantation in a Patient with Recurrent Underweight following Clinical Recovery from Anorexia Nervosa. *Psychother. Psychosom.* **88**, 58–60 (2019).
15. Prochazkova, P. *et al.* Microbiota, Microbial Metabolites, and Barrier Function in A Patient with Anorexia Nervosa after Fecal Microbiota Transplantation. *Microorganisms* **7**, (2019).
16. Hata, T. *et al.* The Gut Microbiome Derived From Anorexia Nervosa Patients Impairs Weight Gain and Behavioral Performance in Female Mice. *Endocrinology* **160**, 2441–2452 (2019).
17. Winter, G., Hart, R. A., Charlesworth, R. P. G. & Sharpley, C. F. Gut microbiome and depression: what we know and what we need to know. *Rev. Neurosci.* **29**, 629–643 (2018).
18. Kelly, J. R. *et al.* Transferring the blues: Depression-associated gut microbiota induces neurobehavioural changes in the rat. *J. Psychiatr. Res.* **82**, 109–118 (2016).
19. Neufeld, K. M., Kang, N., Bienenstock, J. & Foster, J. A. Reduced anxiety-like behavior and central neurochemical change in germ-free mice. *Neurogastroenterol. Motil.* **23**, 255-e119 (2011).
20. Schalla, M. A. & Stengel, A. Activity Based Anorexia as an Animal Model for Anorexia Nervosa–A Systematic Review. *Front. Nutr.* **6**, (2019).
21. Nobis, S. *et al.* Alterations of proteome, mitochondrial dynamic and autophagy in the hypothalamus during activity-based anorexia. *Sci. Rep.* **8**, 7233 (2018).

22. Scharner, S. *et al.* Activity-based anorexia activates nesfatin-1 immunoreactive neurons in distinct brain nuclei of female rats. *Brain Res.* **1677**, 33–46 (2017).
23. Scharner, S. *et al.* Activity-based anorexia activates CRF immunoreactive neurons in female rats. *Neurosci. Lett.* **674**, 142–147 (2018).
24. Kinzig, K. P. & Hargrave, S. L. Adolescent activity-based anorexia increases anxiety-like behavior in adulthood. *Physiol. Behav.* **101**, 269–276 (2010).
25. Belmonte, L. *et al.* A role for intestinal TLR4-driven inflammatory response during activity-based anorexia. *Sci. Rep.* **6**, 1–14 (2016).
26. Jésus, P. *et al.* Alteration of intestinal barrier function during activity-based anorexia in mice. *Clin. Nutr.* **33**, 1046–1053 (2014).
27. Breton, J. *et al.* Gut microbiota alteration in a mouse model of Anorexia Nervosa. *Clin. Nutr. Edinb. Scotl.* (2020).
28. Achamrah, N. *et al.* Sex differences in response to activity-based anorexia model in C57Bl/6 mice. *Physiol. Behav.* **170**, 1–5 (2017).
29. Hapfelmeier, S. *et al.* Reversible Microbial Colonization of Germ-Free Mice Reveals the Dynamics of IgA Immune Responses. *Science* **328**, 1705–1709 (2010).
30. Tirelle, P. *et al.* Comparison of different modes of antibiotic delivery on gut microbiota depletion efficiency and body composition in mouse. *under review*.
31. Ghouzali, I. *et al.* Targeting immunoproteasome and glutamine supplementation prevent intestinal hyperpermeability. *Biochim. Biophys. Acta Gen. Subj.* **1861**, 3278–3288 (2017).
32. Coëffier, M. *et al.* INFLUENCE OF GLUTAMINE ON CYTOKINE PRODUCTION BY HUMAN GUT IN VITRO. *Cytokine* **13**, 148–154 (2001).
33. Feng, Y. *et al.* Antibiotics induced intestinal tight junction barrier dysfunction is associated with microbiota dysbiosis, activated NLRP3 inflammasome and autophagy. *PLoS ONE* **14**, (2019).

34. Steinhausen, H.-C. & Jensen, C. M. Time trends in lifetime incidence rates of first-time diagnosed anorexia nervosa and bulimia nervosa across 16 years in a danish nationwide psychiatric registry study. *Int. J. Eat. Disord.* **48**, 845–850 (2015).
35. Ruusunen, A., Rocks, T., Jacka, F. & Loughman, A. The gut microbiome in anorexia nervosa: relevance for nutritional rehabilitation. *Psychopharmacology (Berl.)* **236**, 1545–1558 (2019).
36. Queipo-Ortuño, M. I. *et al.* Gut microbiota composition in male rat models under different nutritional status and physical activity and its association with serum leptin and ghrelin levels. *PloS One* **8**, e65465 (2013).
37. Cho, I. *et al.* Antibiotics in early life alter the murine colonic microbiome and adiposity. *Nature* **488**, 621–626 (2012).
38. Manickam, R., Oh, H. Y. P., Tan, C. K., Paramalingam, E. & Wahli, W. Metronidazole Causes Skeletal Muscle Atrophy and Modulates Muscle Chronometabolism. *Int. J. Mol. Sci.* **19**, (2018).
39. Ceylani, T., Jakubowska-Doğru, E., Gurbanov, R., Teker, H. T. & Gozen, A. G. The effects of repeated antibiotic administration to juvenile BALB/c mice on the microbiota status and animal behavior at the adult age. *Heliyon* **4**, e00644 (2018).
40. Sylvia, K. E., Jewell, C. P., Rendon, N. M., St John, E. A. & Demas, G. E. Sex-specific modulation of the gut microbiome and behavior in Siberian hamsters. *Brain. Behav. Immun.* **60**, 51–62 (2017).
41. Survival of Starvation by Germfree Mice. *Nutr. Rev.* **26**, 249–251 (1968).
42. Lahiri, S. *et al.* The gut microbiota influences skeletal muscle mass and function in mice. *Sci. Transl. Med.* **11**, (2019).
43. Lian, Q. *et al.* Anorexia nervosa, depression and suicidal thoughts among Chinese adolescents: a national school-based cross-sectional study. *Environ. Health Prev. Med.* **22**, 1–7 (2017).
44. Swinbourne, J. M. & Touyz, S. W. The co-morbidity of eating disorders and anxiety disorders: a review. *Eur. Eat. Disord. Rev.* **15**, 253–274 (2007).
45. Cryan, J. F. *et al.* The Microbiota-Gut-Brain Axis. *Physiol. Rev.* **99**, 1877–2013 (2019).

46. De Palma, G. *et al.* Transplantation of fecal microbiota from patients with irritable bowel syndrome alters gut function and behavior in recipient mice. *Sci. Transl. Med.* **9**, (2017).
47. Zhao, Z. *et al.* Long-Term Exposure to Ceftriaxone Sodium Induces Alteration of Gut Microbiota Accompanied by Abnormal Behaviors in Mice. *Front. Cell. Infect. Microbiol.* **10**, (2020).
48. Lurie, I., Yang, Y.-X., Haynes, K., Mamtani, R. & Boursi, B. Antibiotic exposure and the risk for depression, anxiety, or psychosis: a nested case-control study. *J. Clin. Psychiatry* **76**, 1522–1528 (2015).
49. Trinh, S. *et al.* Gut microbiota and brain alterations in a translational anorexia nervosa rat model. *J. Psychiatr. Res.* **133**, 156–165 (2021).
50. Breton, J. *et al.* Characterizing the metabolic perturbations induced by activity-based anorexia in the C57Bl/6 mouse using 1H NMR spectroscopy. *Clin. Nutr.* (2019).
51. Collins, S. M., Surette, M. & Bercik, P. The interplay between the intestinal microbiota and the brain. *Nat. Rev. Microbiol.* **10**, 735–742 (2012).
52. Mir, H.-D. *et al.* The gut microbiota metabolite indole increases emotional responses and adrenal medulla activity in chronically stressed male mice. *Psychoneuroendocrinology* **119**, 104750 (2020).
53. Dominique, M. *et al.* Changes in Microbiota and Bacterial Protein Caseinolytic Peptidase B During Food Restriction in Mice: Relevance for the Onset and Perpetuation of Anorexia Nervosa. *Nutrients* **11**, (2019).
54. Breton, J. *et al.* Host Starvation and Female Sex Influence Enterobacterial ClpB Production: A Possible Link to the Etiology of Eating Disorders. *Microorganisms* **8**, (2020).

Table 1: Primer sequences for qPCR

Gene	Forward primer	Reverse primer
RPS18	TGCGAGTACTCAACACCAACA	TTCCTCAACACCACATGAGC
NPY	CTGCGACACTACATCAATCT	CTTCAAGCCTTGTTCTGG
POMC	CCTCCTGCTTCAGACCTCCA	GGCTGTTCATCTCCGTTGC
CRH	AGAAGAGAGCGCCCCTAAC	ATCAGAACCGGCTGAGGTTG
DRD1	GTAGCCATTATGATCGTCAC	GATCACAGACAGTGTCTTCAG
DRD2	CTGGAGAGGCAGAACTGGA	TAGACGACCCAGGGCATAAC
HTR1a	TACGTGAACAAGAGGACGCC	AAAGCGCCGAAAGTGGAGTA
HTR4	GGGTTCTGCGCTAAAGGTGG	GCTCCTGGGGTTCTGATCTC
TNFα	TGTCTACTCCTCAGAGCCCC	TGAGTCCTTGATGGTGGTGC
BDNF	TGTGACAGTATTAGCGAGTGGG	TACGATTGGGTAGTTCGGCATT

Figure legends

Figure 1: Faecal bacteria depletion induced by antibiotics in male mice.

Qquantification of bacterial density in mouse faeces at day 0 (d0) and day 15 (d15) in ATB-treated control (CT, open bars) and ATB-treated ABA (blue bars) male mice. Exact p-values are displayed in Supplemental table 1. Results of Bonferroni posthoc tests are shown: ***, p<0.001 vs day 0.

Figure 2: Body weight changes, body composition and anticipatory activity in male mice.

Body weight changes from day 16 to day 28 (**A.**), in control (CT, closed circles), ATB-treated CT (open circles), and in ABA (closed triangles) and ATB-treated ABA (open triangles) male mice. Body weight changes at day 28 (**B.**), fat mass (**C.**), lean mass (**D.**) and anticipatory activity (**E.**). Column bar graphs show CT and ATB-treated CT male mice (open bars) and ABA and ATB-treated ABA male mice (blue bars). In each panel, the boxed text represents the results of the 2-way ANOVA (n=6-8/per group for body composition and n=13-16/per group for anticipatory activity). The p-value of the underlined and bold factor is lower than 0.05. Exact p-values are displayed in Supplemental table 1. Results of Bonferroni posthoc tests are shown: *, p<0.05 vs CT or ATB-treated CT, $^{\#}$, p<0.05 vs untreated (no ATB) mice and $^{\$}$, p<0.05 vs day 5.

Figure 3: Plasma leptin, adiponectin and FITC-dextran concentrations in male mice. Plasma Leptin (**A.**), adiponectin (**B.**) and FITC-dextran 4kDa (**C.**) levels measured at day 28 in control (CT) and ATB-treated CT male mice (open bars) and in ABA and ATB-treated ABA male mice (blue bars). In each panel, the boxed text represents the results of the 2-way ANOVA (n=13-16/per group for leptin and adiponectin n=6-8/group for FITC-dextran). The p-value of the underlined and bold factor is lower than 0.05. Exact p values are displayed in Supplemental table 1. Results of Bonferroni posthoc tests are shown: *, p<0.05 vs CT or ATB-treated CT mice.

Figure 4: Hypothalamic pro-opiomelanocortin (POMC) and neuropeptide Y (NPY) mRNA expression in male mice.

NPY (**A.**) and POMC (**B.**) mRNA expression at day 28 in control (CT) and ATB-treated CT (open bars) and in ABA and ATB-treated ABA (blue bars). In each panel, the boxed text represents the results of the 2-way ANOVA (n=13-16/per group). The p-value of the underlined and bold factor is lower than 0.05. Exact p-values are displayed in Supplemental table 1. Results of Bonferroni posthoc tests are shown: *, p<0.05 CT vs ABA, $^{\#}$, p<0.05 ATB-treated CT vs ATB-treated ABA mice.

Figure 5: Results of Open field test and quantification of hypothalamic cortico-releasing hormone (CRH) mRNA levels in male mice.

Time (**A.**) travelled distance (**B.**), and travelled distance over time ratio (**C.**) at the center of the open field area measured at day 27 in control (CT) and ATB-treated CT (open bars) and in ABA and ATB-treated ABA (blue bars) male mice. Time (**D.**) travelled distance (**E.**) and travelled distance over time ratio (**F.**) at the periphery of the open field area measured at day 27. Immobility time (**G.**) and vertical activity (**H.**) measured during the open filed test at day 27. Quantification of hypothalamic CRH (**I.**) mRNA expression at day 28 in male mice. In each panel, the boxed text represents the results of the 2-way ANOVA (n=6-8/per group for open field test and n=13-16/per group for CRH quantification). The p-value of the underlined and bold factor is lower than 0.05. Exact p values are displayed in Supplemental table 1. Results of Bonferroni posthoc tests are shown: *, $p<0.05$ vs CT or ATB-treated CT, $^{\#}$, $p<0.05$ vs untreated (no ATB) mice.

Figure 6: Hippocampal dopaminergic receptor 1 (DRD1) and 2 (DRD2), serotoninergic receptor 1 (5-HT1A) and 4 (5-HT4), tumor necrosis factors α (TNFα) and brain-derived neurotrophic factor (BDNF) mRNA expression in male mice.

DRD1 (**A.**) DRD2 (**B.**) 5-HT1A (**C.**) 5-HT4 (**D.**) TNFα (**E.**) and BDNF (**F.**) mRNA expression at day 28 in control (CT) and ATB-treated CT (open bars) and in ABA and ATB-treated ABA (blue bars) male mice. In each panel, the boxed text represents the results of the 2-way ANOVA (n=13-16/per group). The p-value of the underlined and bold factor is lower than 0.05. Exact p-values are displayed in Supplemental table 1. Results of Bonferroni posthoc tests are shown: *, $p<0.05$ CT vs ABA, $^{\#}$, $p<0.05$ ATB-treated CT vs ATB-treated ABA mice.

Figure 7: Body weight changes, body composition and anticipatory activity in female mice.

Body weight changes from day 16 to day 28 (**A.**), in control (CT, closed circles), ATB-treated CT (open circles), ABA (closed triangles) and in ATB-treated ABA (open triangles) female mice. Body weight changes (**B.**) at day 27, fat mass (**C.**), lean mass (**D.**) and anticipatory activity (**E.**). Column bar graphs show CT and ATB-treated CT female mice (open bars) and ABA and ATB-treated ABA female mice (red bars). In each panel, the boxed text represents the results of the 2-way ANOVA (n=6-8/per group). The p-value of the underlined and bold factor is lower than 0.05. Exact p-values are displayed in Supplemental table 1. Results of Bonferroni posthoc tests are shown: *, $p<0.05$ vs CT or ATB-treated CT, $^{\#}$, $p<0.05$ vs untreated (no ATB) mice and $^{\$}$, $p<0.05$ vs day 5.

Figure 8: Plasma leptin, adiponectin and FITC-dextran concentrations in female mice.

Plasma Leptin (**A.**), adiponectin (**B.**) and FITC-dextran 4kDa (**C.**) levels measured at day 28 in control (CT) and ATB-treated CT female mice (open bars) and in ABA and ATB-treated ABA female mice (red bars). In each panel, the boxed text represents the results of the 2-way ANOVA (n=6-8/per group). The p-value of the underlined and bold factor is lower than 0.05. Exact p-values are displayed in Supplemental table 1. Results of Bonferroni posthoc tests are shown: *, $p<0.05$ vs CT or ATB-treated CT, $^{\#}$, $p<0.05$ vs untreated (no ATB) mice.

Figure 9: Results of Open field test and hypothalamic cortico-releasing hormone (CRH) mRNA expression in female mice.

Time (**A.**) travelled distance (**B.**), and travelled distance over time ratio (**C.**) at the center of the open field area measured at day 27 in control (CT) and ATB-treated CT (open bars) and in ABA and ATB-treated ABA (blue bars) female mice. Time (**D.**) travelled distance (**E.**) and travelled distance over time ratio (**F.**) at the periphery of the open field area measured at day 27. Immobility time (**G.**) and vertical activity (**H.**) measured during the open filed test at day 27. Quantification of hypothalamic CRH (**I.**) mRNA expression at day 28 in female mice. In each panel, the boxed text represents the results of the 2-way ANOVA (n=6-8/per group for open field test and for CRH quantification). The p-value of the underlined and bold factor is lower than 0.05. Exact p-values are displayed in Supplemental table 1. Results of Bonferroni posthoc tests are shown: *, $p<0.05$ vs CT or ATB-treated CT.

Figure 1

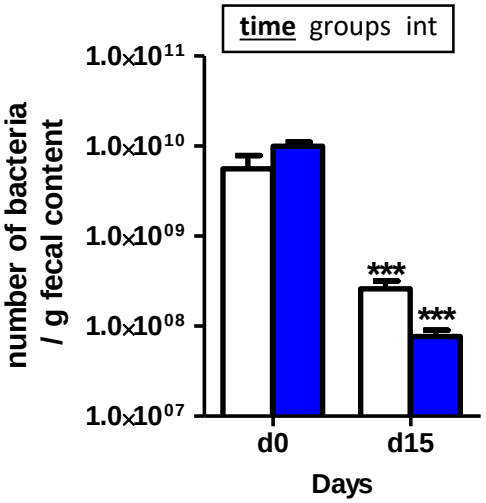
time groups int
number of bacteria / g fecal content
1.0x10^11
1.0x10^10
1.0x10^09
1.0x10^08
1.0x10^07
***
***
d0
d15
Days

Figure 2

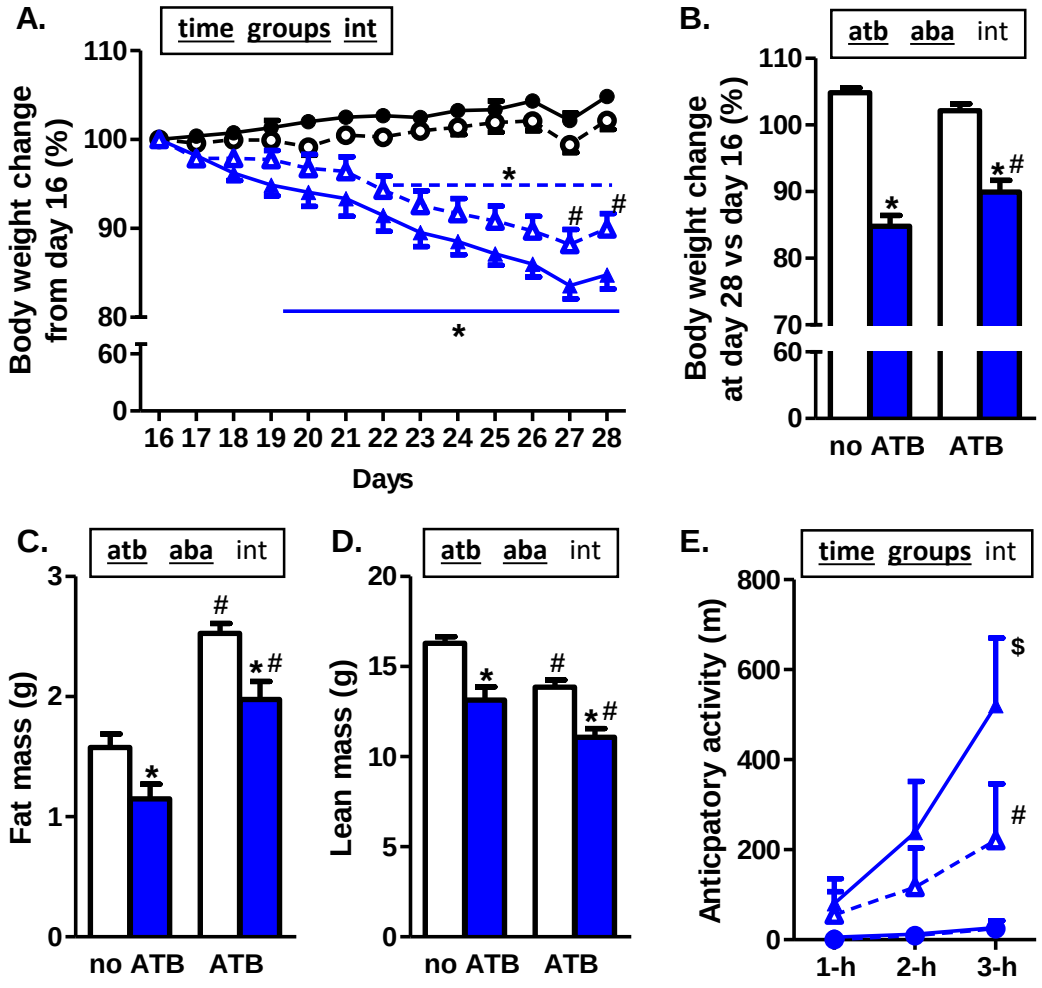
A.
time groups int
Body weight change from day 16 (%)
110
100
90
80
60
0
16 17 18 19 20 21 22 23 24 25 26 27 28
Days
*
#
#
*
B.
atb aba int
Body weight change at day 28 vs day 16 (%)
110
100
90
80
70
60
0
*
*#
no ATB
ATB
C.
atb aba int
Fat mass (g)
3
2
1
0
*
#
*#
no ATB
ATB
D.
atb aba int
Lean mass (g)
20
15
10
5
0
*
#
*#
no ATB
ATB
E.
time groups int
Anticpatory activity (m)
800
600
400
200
0
$
#
1-h
2-h
3-h

Figure 3

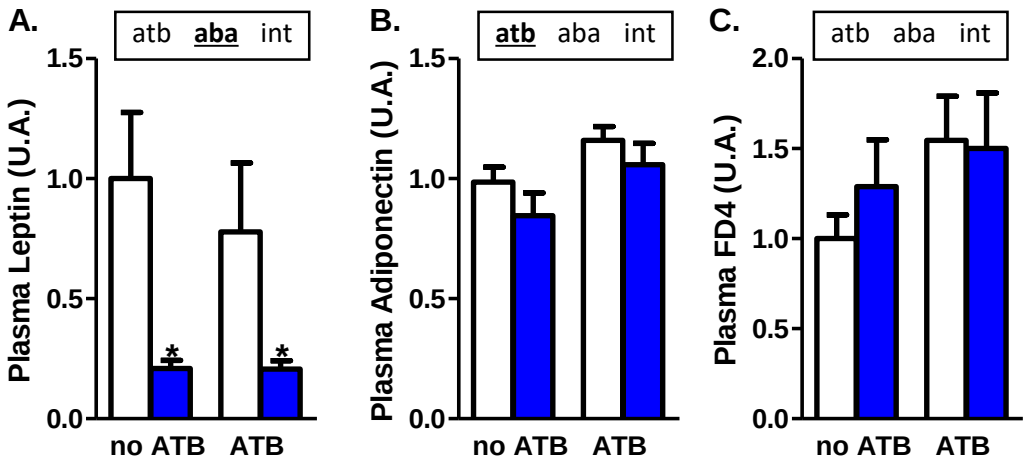
A.
atb aba int
Plasma Leptin (U.A.)
1.5
1.0
0.5
0.0
*
*
no ATB
ATB
B.
atb aba int
Plasma Adiponectin (U.A.)
1.5
1.0
0.5
0.0
no ATB
ATB
C.
atb aba int
Plasma FD4 (U.A.)
2.0
1.5
1.0
0.5
0.0
no ATB
ATB

Figure 4

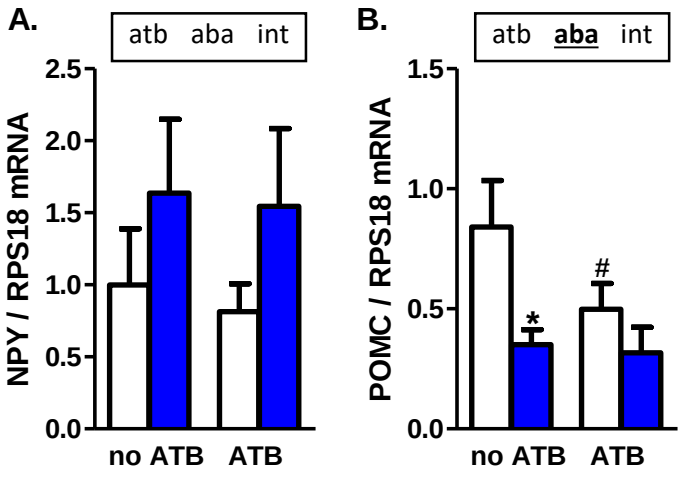
A.
atb aba int
NPY / RPS18 mRNA
2.5
2.0
1.5
1.0
0.5
0.0
no ATB
ATB
B.
atb aba int
POMC / RPS18 mRNA
1.5
1.0
0.5
0.0
*
#
no ATB
ATB

Figure 5

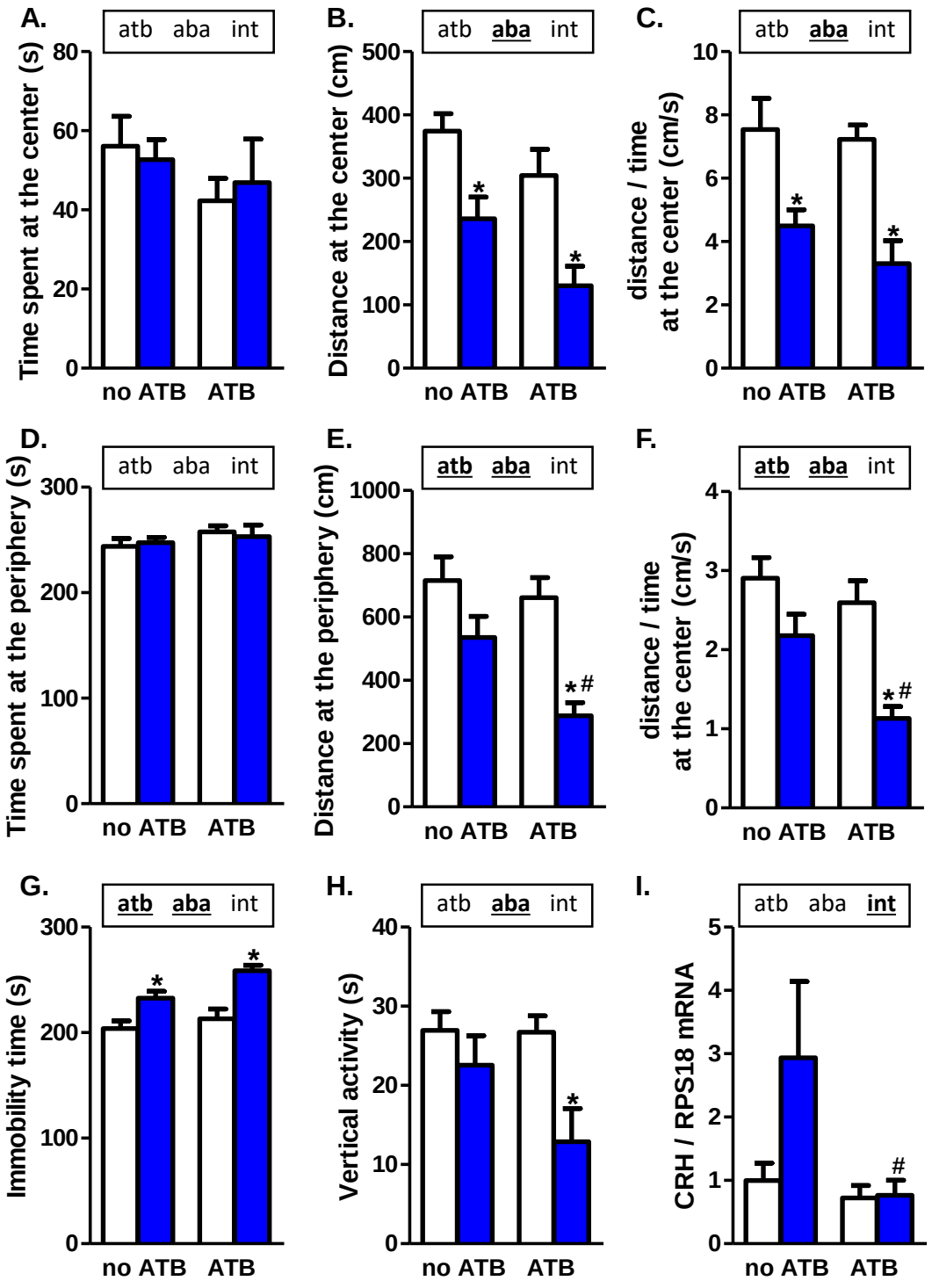
A.
atb aba int
Time spent at the center (s)
0
20
40
60
80
no ATB
ATB
B.
atb aba int
Distance at the center (cm)
0
100
200
300
400
500
*
*
no ATB
ATB
C.
atb aba int
distance / time at the center (cm/s)
0
2
4
6
8
10
*
*
no ATB
ATB
D.
atb aba int
Time spent at the periphery (s)
0
100
200
300
no ATB
ATB
E.
atb aba int
Distance at the periphery (cm)
0
200
400
600
800
1000
*#
no ATB
ATB
F.
atb aba int
distance / time at the center (cm/s)
0
1
2
3
4
*#
no ATB
ATB
G.
atb aba int
Immobility time (s)
0
100
200
300
*
*
no ATB
ATB
H.
atb aba int
Vertical activity (s)
0
10
20
30
40
*
no ATB
ATB
I.
atb aba int
CRH / RPS18 mRNA
0
1
2
3
4
5
#
no ATB
ATB

Figure 6

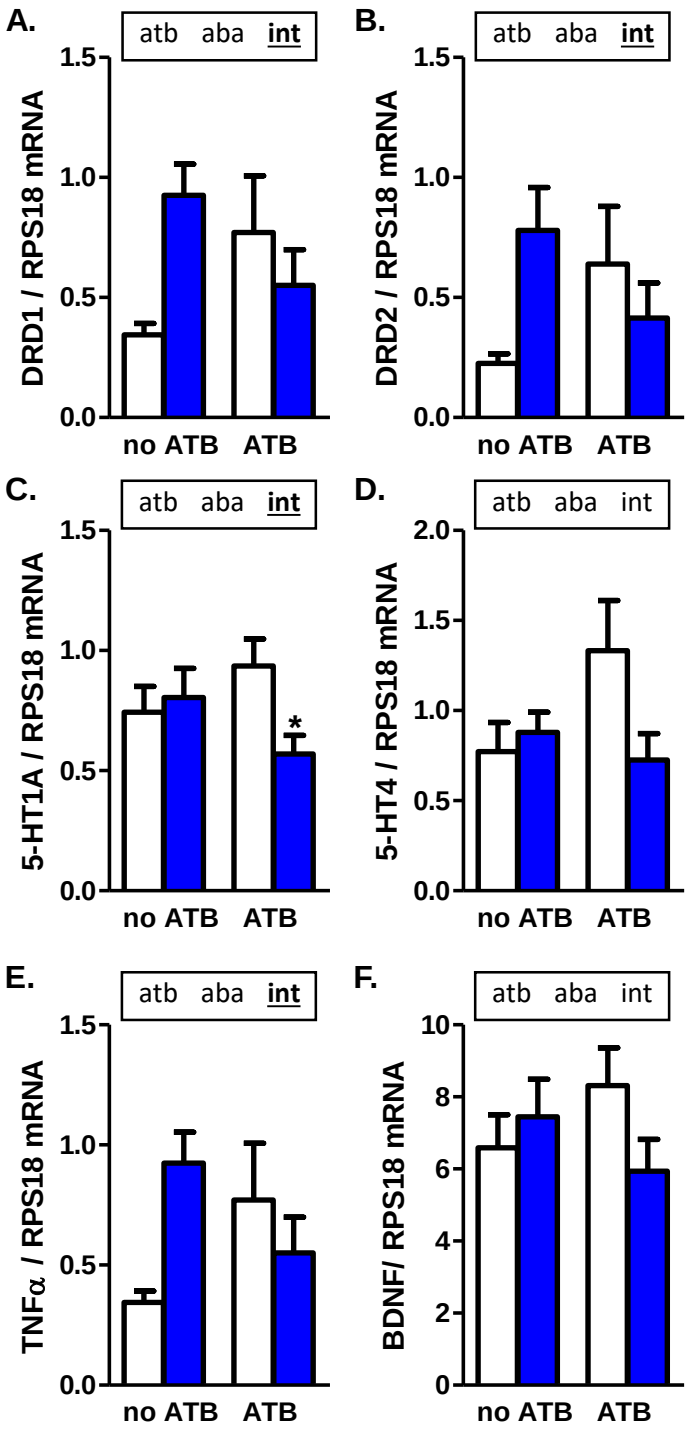
A.
atb aba int
DRD1 / RPS18 mRNA
1.5
1.0
0.5
0.0
no ATB
ATB
B.
atb aba int
DRD2 / RPS18 mRNA
1.5
1.0
0.5
0.0
no ATB
ATB
C.
atb aba int
5-HT1A / RPS18 mRNA
1.5
1.0
0.5
0.0
*
no ATB
ATB
D.
atb aba int
5-HT4 / RPS18 mRNA
2.0
1.5
1.0
0.5
0.0
no ATB
ATB
E.
atb aba int
TNFα / RPS18 mRNA
1.5
1.0
0.5
0.0
no ATB
ATB
F.
atb aba int
BDNF/ RPS18 mRNA
10
8
6
4
2
0
no ATB
ATB

Figure 7

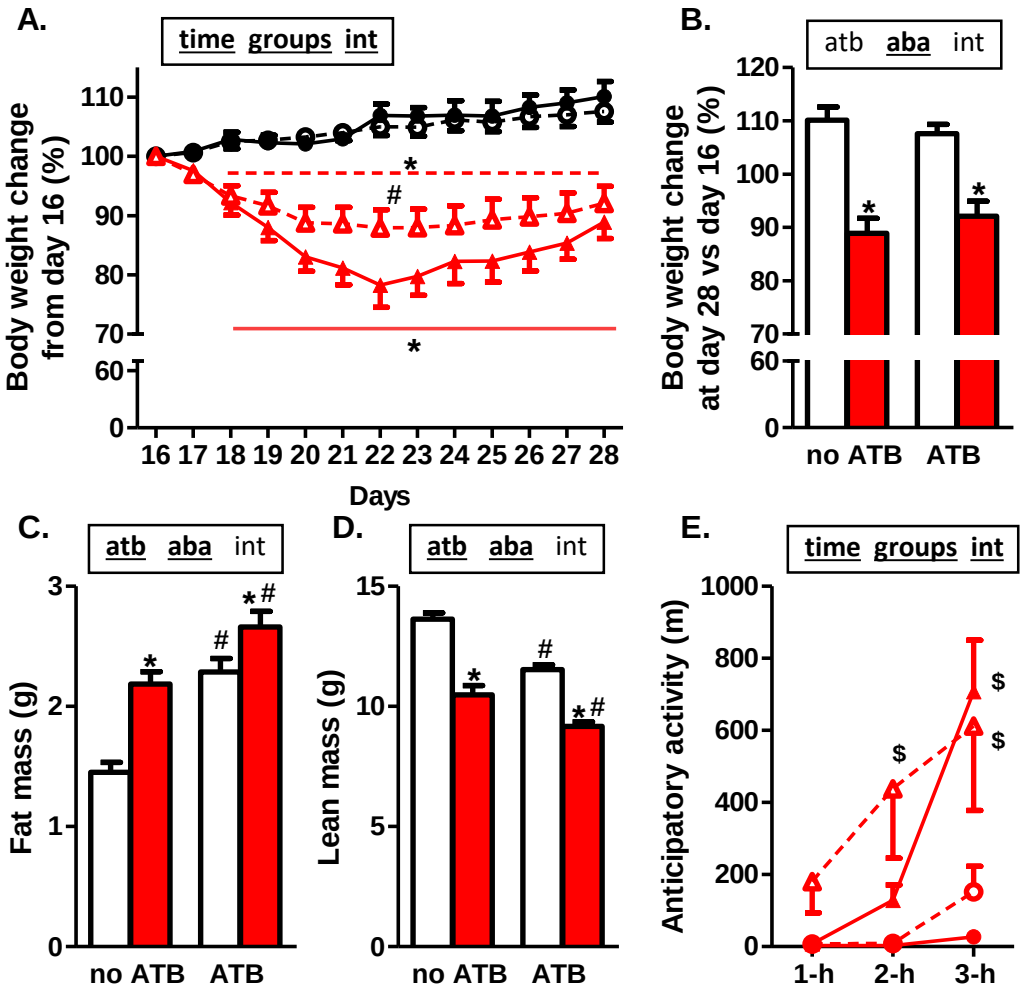
A.
time groups int
Body weight change from day 16 (%)
Days
B.
atb aba int
Body weight change at day 28 vs day 16 (%)
no ATB
ATB
C.
atb aba int
Fat mass (g)
D.
atb aba int
Lean mass (g)
E.
time groups int
Anticipatory activity (m)
1-h
2-h
3-h

Figure 8

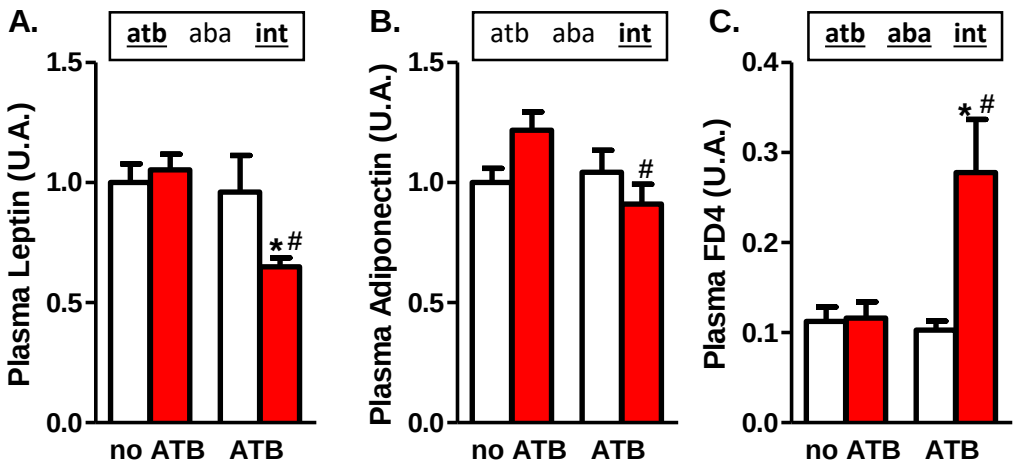
A.
atb aba int
Plasma Leptin (U.A.)
1.5
1.0
0.5
0.0
*#
no ATB
ATB
B.
atb aba int
Plasma Adiponectin (U.A.)
1.5
1.0
0.5
0.0
#
no ATB
ATB
C.
atb aba int
Plasma FD4 (U.A.)
0.4
0.3
0.2
0.1
0.0
*#
no ATB
ATB

Figure 9

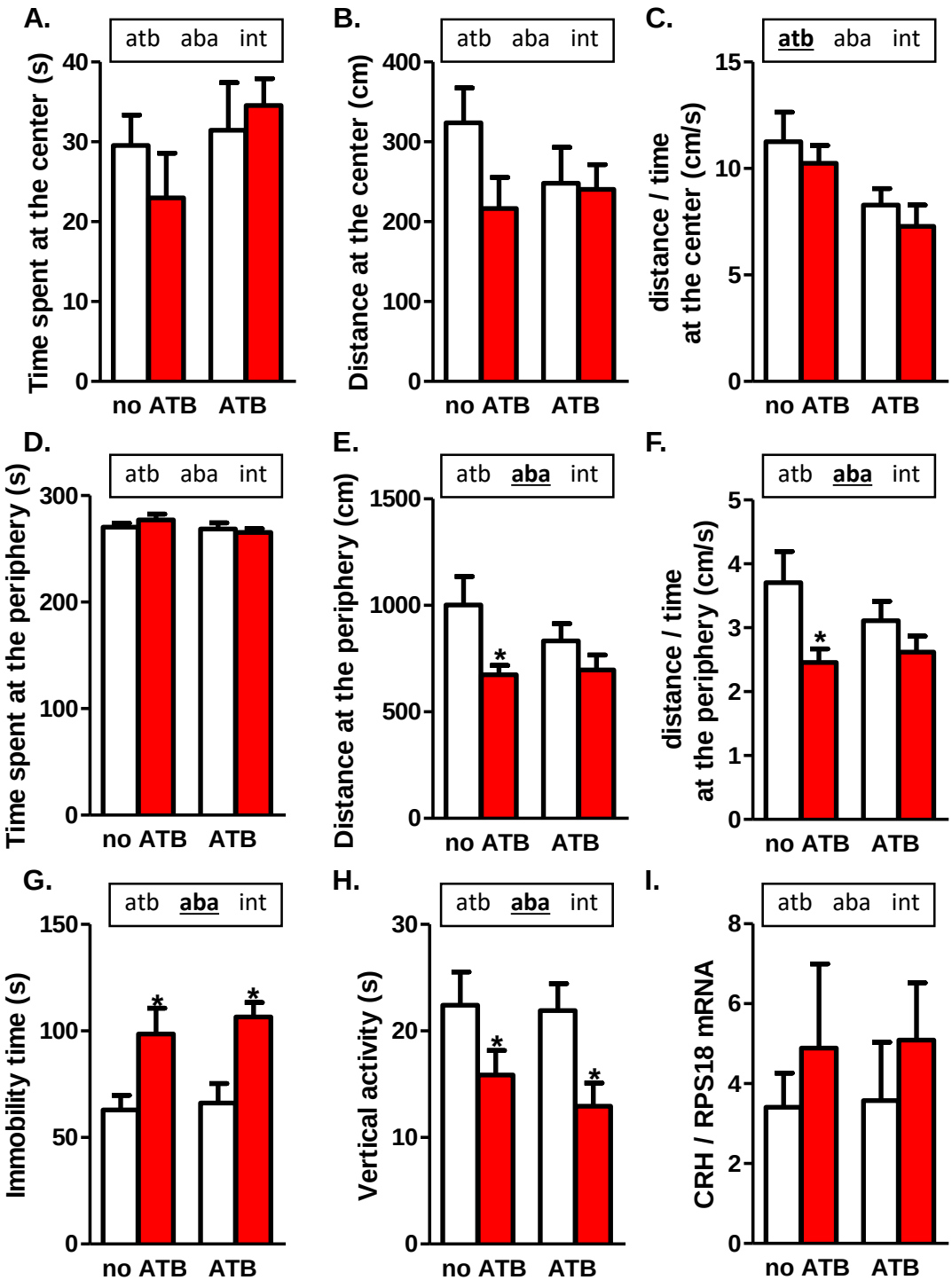
A.
atb aba int
Time spent at the center (s)
40
30
20
10
0
no ATB ATB
B.
atb aba int
Distance at the center (cm)
400
300
200
100
0
no ATB ATB
C.
atb aba int
distance / time at the center (cm/s)
15
10
5
0
no ATB ATB
D.
atb aba int
Time spent at the periphery (s)
300
200
100
0
no ATB ATB
E.
atb aba int
Distance at the periphery (cm)
1500
1000
500
0
*
no ATB ATB
F.
atb aba int
distance / time at the periphery (cm/s)
5
4
3
2
1
0
*
no ATB ATB
G.
atb aba int
Immobility time (s)
150
100
50
0
* *
no ATB ATB
H.
atb aba int
Vertical activity (s)
30
20
10
0
* *
no ATB ATB
I.
atb aba int
CRH / RPS18 mRNA
8
6
4
2
0
no ATB ATB